Sensors and Materials, Vol. 36, No. 2 (2024) 473–479
MYU Tokyo

S & M 3534

Photoluminescence and Scintillation Properties of Eu:$CaHfO_3$ Single Crystals

Yusuke Endo,* Kensei Ichiba, Daisuke Nakauchi,
Takumi Kato, Noriaki Kawaguchi, and Takayuki Yanagida

Division of Materials Science, Nara Institute of Science and Technology,
Takayama, Ikoma, Nara 630-0192, Japan

(Received October 20, 2023; accepted January 23, 2024)

Keywords: scintillator, radiation detector, photoluminescence, $CaHfO_3$

Eu:$CaHfO_3$ single crystals with various Eu concentrations were synthesized by the floating zone method, and their photoluminescence (PL) and scintillation properties were investigated. All the samples showed PL peaks at 590, 620, and 650 nm, which were due to the 4f-4f transitions of Eu^{3+}. The PL quantum yield of 1.0% Eu:$CaHfO_3$ was the highest at 42.2% among the samples. The X-ray-induced scintillation spectra showed several emission peaks in the range of 400–690 nm, and the emissions were attributed to the 4f-4f transitions of Eu^{3+}. Among the samples, 0.05% Eu:$CaHfO_3$ showed the highest intensity. In the afterglow curves, the levels were within the range of 1,000–10,000 ppm and those of previous studies.

1. Introduction

Inorganic scintillators can absorb ionizing radiation with high energy to momentarily convert it into photons with low energy.[1–3] Taking advantage of this feature, the scintillators have been applied to radiation detectors by combining them with photodetectors that can convert the photons into electrical signals.[4,5] The scintillation detectors are classified into current and photon counting mode measurements depending on their application.[6,7] In particular, the detectors for the current mode type integrate the signal for a period of milliseconds and have been used in applications such as X-ray computed tomography (CT) and flat panel detectors for X-ray radiography.[8] The scintillators for the current mode type require properties such as high emission intensity, a large effective atomic number (Z_{eff}), high density (ρ), and low afterglow level (AL). However, since no scintillators satisfy all the required properties, new scintillators have been developed.[9–14]

HfO_2-based compounds such as $RE_2Hf_2O_7$ (RE = La, Gd, Lu) and $AEHfO_3$ (AE = Ca, Sr, Ba) have attracted attention as candidates for scintillators owing to their large Z_{eff} and high ρ. In previous reports on HfO_2-based scintillators, only $CaHfO_3$ with Z_{eff} (65.2) and ρ (6.95 g/cm^3) showed a scintillation light yield above 10,000 photons/MeV.[15–21] Moreover, our research group has investigated the scintillation properties of $CaHfO_3$ doped with Ti, Ce, Pr, Tb, and Tm,[18,21–26]

*Corresponding author: e-mail: endo.yusuke.ey5@ms.naist.jp
https://doi.org/10.18494/SAM4758

ISSN 0914-4935

and $CaHfO_3$ doped with various rare-earth elements was found to show high luminescence properties.

Eu^{3+} is used as a luminescence center for red scintillators, and the emission wavelength is well matched with a Si-based photodetector. A representative Eu^{3+}-doped material, Eu:$(Y,Gd)_2O_3$ ceramic, is used in a commercial scintillator for X-ray CT.[4,27–29] Furthermore, many Eu^{3+}-doped scintillators have been developed in previous studies.[30–38] Therefore, it is considered that Eu^{3+} is useful for scintillators. However, the scintillation properties of Eu:$CaHfO_3$ have not been reported. In this study, Eu:$CaHfO_3$ single crystals were synthesized by the floating zone (FZ) method, and their photoluminescence (PL) and scintillation properties were investigated.

2. Experimental Setup

An FZ furnace with four Xe lamps (Crystal Systems Corporation, FZ-T-12000-X-VPO-PC-YH) was used to synthesize Eu:$CaHfO_3$ single crystals.[16] The Eu concentrations were 0.01, 0.05, 0.1, 0.5, and 1.0 at% with respect to Ca. CaO (99.99%, Furuuchi Chemical), HfO_2 (99.95%, Rare Metallic), and Eu_2O_3 (99.99%, Furuuchi Chemical) were used as starting materials and uniformly blended using a mortar and pestle. To account for Ca evaporation during the crystal growth, CaO was raised by 10% in relation to the stoichiometric composition.[18] The mixtures were placed inside balloons to form cylindrical rods by applying hydrostatic pressure. The rods with different Eu concentrations were subsequently calcined at 1400 °C for 8 h in air using an electric furnace (Crystal Systems, BF-1800-IV-II), and the acquired rods were used for crystallization. During the crystallization, the pull-down speed was 10 mm/h, and the upper and lower rotation rates were 23 rpm to the right and 20 rpm to the left, respectively. The synthesized samples were split, and a grinder polisher (Buehler, MetaServ 250) was used to mechanically polish the surfaces.

A diffractometer (Rigaku, MiniFlex600) equipped with a Cu Kα micro-X-ray tube containing a Be window was used to measure the powder X-ray diffraction (XRD) patterns of the samples in the range of 2θ = 10–70°. Diffuse transmission spectra were measured using a spectrophotometer (Shimadzu, Solidspec-3700).

Three-dimensional PL excitation and emission spectra and quantum yield (*QY*) were measured using Quantaurus-QY (Hamamatsu Photonics, C11347). The measurement ranges of emission and excitation wavelengths were 300–800 nm and 250–400 nm, respectively. Quantaurus-τ (Hamamatsu Photonics, C11367) was used to evaluate PL decay time profiles. X-ray-induced scintillation spectra were measured using our original setup.[39] The X-ray-induced scintillation decay and afterglow curves were evaluated using our original measurement system.[40]

3. Results and Discussion

Figure 1 shows a photograph of the 0.01, 0.05, 0.1, 0.5, and 1.0% Eu:$CaHfO_3$ single crystals. All the samples looked colorless and transparent. Additionally, the length, width, and thickness of the 0.01, 0.05, 0.1, 0.5, and 1.0% Eu:$CaHfO_3$ were approximately 4 × 4 × 0.75 mm^3. Figure 2

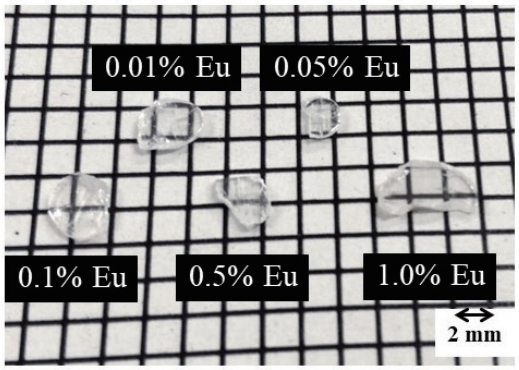

Fig. 1. (Color online) Photograph of Eu:$CaHfO_3$ single crystals.

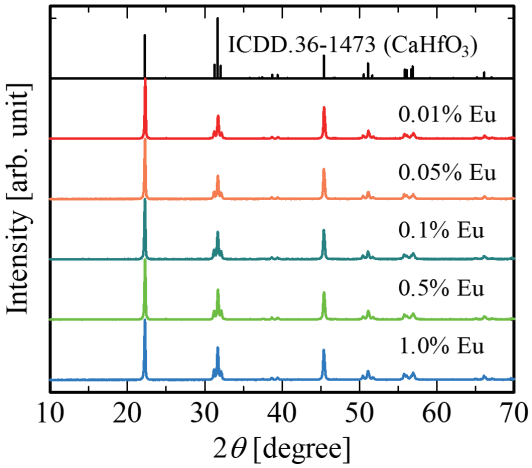

Fig. 2. (Color online) Powder XRD patterns of Eu:$CaHfO_3$ single crystals and reference data.

shows the powder XRD patterns of the Eu:$CaHfO_3$ single crystals and the reference data from International Crystallographic Diffraction Data (ICDD) No. 36-1473. The diffraction peaks of the samples were observed at the same positions as those of the reference data, and no impurity phases were detected. Hence, the synthesized samples had a single-phase structure of $CaHfO_3$.[41,42]

Figure 3 shows the diffuse transmission spectra of Eu:$CaHfO_3$ in the wavelength range of 200 to 850 nm. In the 300–850 nm range, Eu:$CaHfO_3$ showed the maximum transmittance at approximately 70–80%, and the transmittances of the 0.05 and 0.5% doped samples were slightly lower than those of the other samples. The decrease in the transmittance arose from the presence of cracks, as shown in Fig. 1. Absorption attributed to the charge transfer of Eu^{3+}–O^{2-} was observed in all the samples at wavelengths shorter than 300 nm.[43]

Figure 4 shows the three-dimensional PL excitation and emission spectrum of the 1.0% Eu:$CaHfO_3$ as a typical sample. This Eu:$CaHfO_3$ showed the three emission peaks at 590, 620, and 690 nm originating from the 4f-4f transitions of Eu^{3+}.[44,45] A similar trend was observed in other samples. The PL *QY*s in the range of 550–750 nm under the 300 nm excitation wavelength of 0.01, 0.05, 0.1, 0.5, and 1.0% Eu:$CaHfO_3$ were 1.5, 4.6, 12.2, 32.6, and 42.2%, respectively. The increase in PL *QY* is attributed to an increase in Eu concentration, and no concentration quenching was observed in 0.01, 0.05, 0.1, 0.5, and 1.0% Eu:$CaHfO_3$.

Figure 5 shows the PL decay time profiles of 0.01, 0.05, 0.1, 0.5, and 1.0% Eu:$CaHfO_3$ single crystals, where the dashed lines indicate the fitted curves. All the decay curves of the samples were well approximated by a single-exponential function. Each obtained PL decay time constant was 0.96–0.99 ms, which was the range of typical values of the Eu^{3+}-doped materials.[46,47] Hence, the emission of the samples originated from the 4f–4f transitions of Eu^{3+}.

Figure 6 shows the X-ray-induced scintillation spectra of Eu:$CaHfO_3$. All the Eu:$CaHfO_3$ samples showed several emission peaks at 420 nm ($^5D_3$–$^7F_1$), 430 nm ($^5D_3$–$^7F_2$), 450 nm ($^5D_3$–

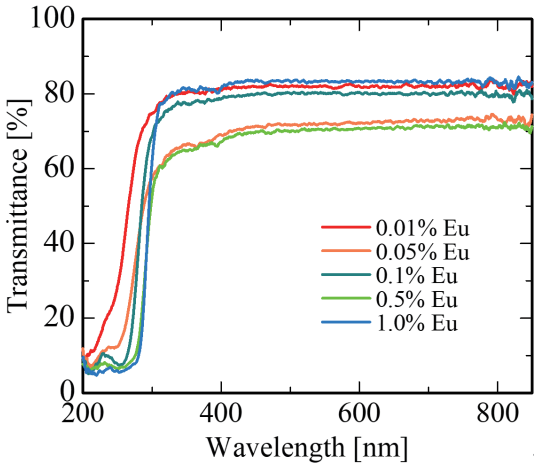

Fig. 3. (Color online) Diffuse transmission spectra of Eu:$CaHfO_3$.

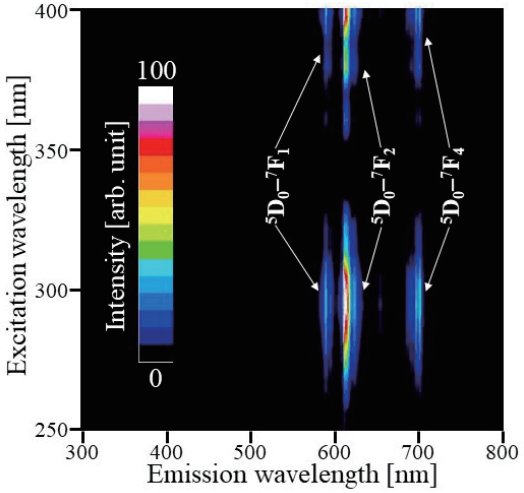

Fig. 4. (Color online) Three-dimensional PL excitation and emission spectrum of 1.0% Eu:$CaHfO_3$.

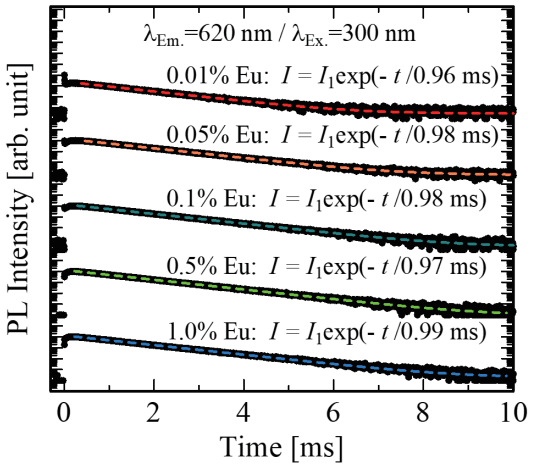

Fig. 5. (Color online) PL decay curves of Eu:$CaHfO_3$. The monitored and excitation wavelengths were 620 and 300 nm, respectively.

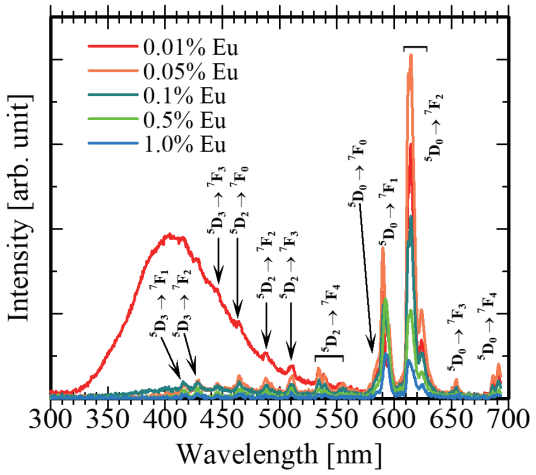

Fig. 6. (Color online) X-ray-induced scintillation spectra of Eu:$CaHfO_3$.

$^7F_3$), 470 nm ($^5D_2$–$^7F_0$), 490 nm ($^5D_2$–$^7F_2$), 510 nm ($^5D_2$–$^7F_3$), 530 nm ($^5D_2$–$^7F_4$), 580 nm ($^5D_0$–$^7F_0$), 590 nm ($^5D_0$–$^7F_1$), 620 nm ($^5D_0$–$^7F_2$), 650 nm ($^5D_0$–$^7F_3$), and 690 nm ($^5D_0$–$^7F_4$) owing to the 4f-4f transitions of Eu^{3+}.[33,35,36,48] In addition, the broad emission band at around 400 nm in 0.01% Eu:$CaHfO_3$ was derived from the host material.[22–25] The highest intensity was observed in 0.05% Eu:$CaHfO_3$, and the trends in PL *QY* and the scintillation intensity were not consistent. Generally, the scintillation intensity depends on PL *QY* and the energy migration efficiency from the host to emission centers.[49] Therefore, the energy migration efficiency was more dominant than PL *QY* in affecting the scintillation properties of Eu:$CaHfO_3$.

Figure 7 shows the X-ray-induced scintillation decay time profiles of Eu:$CaHfO_3$, and the dashed lines show the fitted curves. The obtained decay curves of Eu:$CaHfO_3$ were approximated by a sum of two exponential components except for an instrumental response function (IRF). The first and second components, which were 0.80–1.1 ms and 2.8–3.0 ms, would be attributed to the host emission and the 4f–4f transitions of Eu^{3+},[21,43,50,51] respectively.

Figure 8 shows the afterglow curves of Eu:$CaHfO_3$ samples. *AL* is defined as follows: *AL* [ppm] = $10^6 \times (I_2 - I_{bg})/(I_1 - I_{bg})$, where I_{bg}, I_1, and I_2 are the mean signal intensity in the background, with X-ray irradiation, and at t = 20 ms after irradiation, respectively. The *AL* values of 0.01, 0.05, 0.1, 0.5, and 1.0% Eu:$CaHfO_3$ were 10000, 3800, 4100, 1100, and 1000 ppm with a typical error of 8%, respectively. The obtained values were comparable to those of $CaHfO_3$ crystals doped with other dopant ions.[18,22–24,26] Since general commercial scintillators such as $CdWO_4$ and $Bi_4Ge_3O_{12}$ have an *AL* value of around 10 ppm,[40] the *AL* value of Eu:$CaHfO_3$ was quite high.

4. Conclusions

Eu:$CaHfO_3$ single crystals were synthesized by the FZ method, and their PL and scintillation properties were investigated. PL *QY* was the highest at 42.2% in 1.0% Eu:$CaHfO_3$ under the excitation and emission wavelengths of 300 and 550–750 nm, respectively. The value was higher than those of Ce- and Pr-doped $CaHfO_3$ (32.6% and 6.8%,[18,24] respectively). The scintillation spectra showed several emission peaks from 400 to 690 nm originating from the 4f-4f transitions of Eu^{3+}. 0.05% Eu:$CaHfO_3$ showed the highest emission intensity among the present samples. 0.01% Eu:$CaHfO_3$ showed the lowest *AL* value of 1,000 ppm among the samples, and this value was higher than those of Ce- and Pr-doped $CaHfO_3$ (666 and 228 ppm,[18,24] respectively). The results obtained in this study showed that the material properties of the Eu:$CaHfO_3$ single crystal were inadequate for practical use. On the other hand, previous studies showed that $CaHfO_3$ has excellent scintillation properties.[21,26] Hence, the scintillation properties when using dopants other than Eu and the rare-earth elements considered in previous studies should be evaluated.

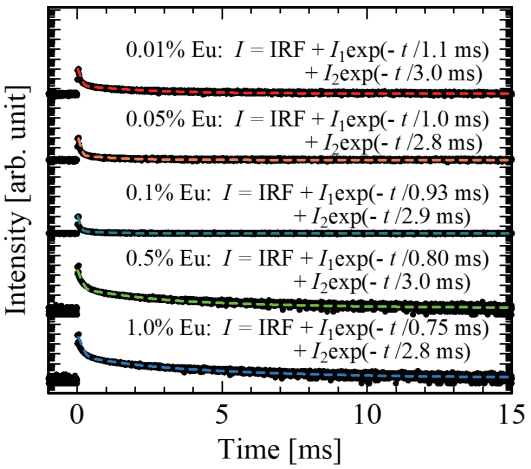

Fig. 7. (Color online) X-ray-induced scintillation decay time profiles of Eu:$CaHfO_3$.

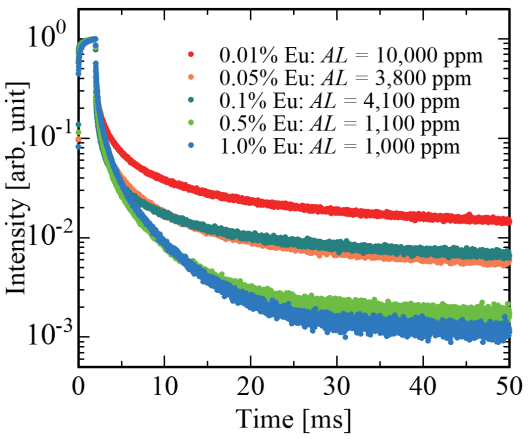

Fig. 8. (Color online) Afterglow curves of Eu:$CaHfO_3$ with 2 ms X-ray irradiation.

Acknowledgments

This work was supported by Grants-in-Aid for Scientific Research A (22H00309), Scientific Research B (22H03872, 22H02939, 21H03733, and 21H03736), Early-Career Scientists (23K13689), and Challenging Exploratory Research (22K18997) from the Japan Society for the Promotion of Science. The Cooperative Research Project of the Research Center for Biomedical Engineering, A-STEP from JST, Kazuchika Okura Memorial Foundation, Asahi Glass Foundation, Nakatani Foundation, and Konica Minolta Science and Technology Foundation are also acknowledged.

References

1 S. E. Derenzo, M. J. Weber, E. Bourret-Courchesne, and M. K. Klintenberg: Nucl. Instrum. Methods Phys. Res., Sect. A **505** (2003) 111. https://doi.org/10.1016/S0168-9002(03)01031-3
2 A. Lempicki, A. J. Wojtowicz, and E. Berman: Nucl. Instrum. Methods Phys. Res., Sect.A **333** (1993) 304. https://doi.org/10.1016/0168-9002(93)91170-R
3 T. Yanagida, T. Kato, D. Nakauchi, and N. Kawaguchi: Jpn. J. Appl. Phys. **62** (2023) 010508. https://doi.org/10.35848/1347-4065/ac9026
4 C. Greskovich and S. Duclos: Annu. Rev. Mater. Sci. **27** (1997) 69. https://doi.org/10.1146/annurev.matsci.27.1.69
5 G. Blasse: Chem. Mater. **6** (1994) 1465. https://doi.org/10.1021/cm00045a002
6 T. Hayashi, K. Ichiba, D. Nakauchi, K. Watanabe, T. Kato, N. Kawaguchi, and T. Yanagida: J. Lumin. **255** (2023) 119614. https://doi.org/10.1016/j.jlumin.2022.119614
7 M. J. Willemink, M. Persson, A. Pourmorteza, N. J. Pelc, and D. Fleischmann: Radiology **289** (2018) 293. https://doi.org/10.1148/radiol.2018172656
8 A. Nassalski, M. Kapusta, T. Batsch, D. Wolski, D. Mockel, W. Enghardt, and M. Moszynski: IEEE Nucl. Sci. Symp. Conf. Record (2005) 2823. https://doi.org/10.1109/NSSMIC.2005.1596921
9 T. Kunikata, T. Kato, D. Shiratori, P. Kantuptim, D. Nakauchi, N. Kawaguchi, and T. Yanagida: Sens. Mater. **35** (2023) 491. https://doi.org/10.18494/SAM4145
10 Y. Takebuchi, D. Shiratori, T. Kato, D. Nakauchi, N. Kawaguchi, and T. Yanagida: Sens. Mater. **35** (2023) 507. https://doi.org/10.18494/SAM4142
11 P. Kantuptim, T. Kato, D. Nakauchi, N. Kawaguchi, K. Watanabe, and T. Yanagida: Sens. Mater. **35** (2023) 451. https://doi.org/10.18494/SAM4141
12 D. Shiratori, H. Fukushima, D. Nakauchi, T. Kato, N. Kawaguchi, and T. Yanagida: Sens. Mater **35** (2023) 439. https://doi.org/10.18494/SAM4140
13 N. Kawaguchi, K. Watanabe, D. Shiratori, T. Kato, D. Nakauchi, and T. Yanagida: Sens. Mater. **35** (2023) 499. https://doi.org/10.18494/SAM4136
14 K. Yamabayashi, K. Okazaki, D. Nakauchi, T. Kato, N. Kawaguchi, and T. Yanagida: Radiat. Phys. Chem. **214** (2024) 111292. https://doi.org/10.1016/j.radphyschem.2023.111292
15 K. Fiaczyk, A. J. Wojtowicz, and E. Zych: J. Phys. Chem. C **119** (2015) 5026. https://doi.org/10.1021/jp512685u
16 D. Nakauchi, G. Okada, N. Kawaguchi, and T. Yanagida: Jpn. J. Appl. Phys. **57** (2018) 100307. https://doi.org/10.7567/JJAP.57.100307
17 D. Nakauchi, T. Kato, N. Kawaguchi, and T. Yanagida: Sens. Mater. **32** (2020) 1389. https://doi.org/10.18494/SAM.2020.2751
18 H. Fukushima, D. Nakauchi, T. Kato, N. Kawaguchi, and T. Yanagida: J. Lumin. **250** (2022) 119088. https://doi.org/10.1016/j.jlumin.2022.119088
19 E. V. van Loef, W. M. Higgins, J. Glodo, C. Brecher, A. Lempicki, V. Venkataramani, W. W. Moses, S. E. Derenzo, and K. S. Shah: 2006 IEEE Nucl. Sci. Symp. Conf. Record (2006) 1538. https://doi.org/10.1109/NSSMIC.2006.354191
20 H. Fukushima, D. Nakauchi, G. Okada, T. Kato, N. Kawaguchi, and T. Yanagida: J. Alloys Compd. **934** (2023) 167929. https://doi.org/10.1016/j.jallcom.2022.167929
21 Y. Endo, K. Ichiba, D. Nakauchi, H. Fukushima, K. Watanabe, T. Kato, N. Kawaguchi, and T. Yanagida: Solid State Sci. **145** (2023) 107333. https://doi.org/10.1016/j.solidstatesciences.2023.107333

22 H. Fukushima, D. Nakauchi, G. Okada, N. Kawaguchi, and T. Yanagida: J. Mater. Sci. Mater. Electron. **29** (2018) 21033. https://doi.org/10.1007/s10854-018-0249-9
23 H. Fukushima, D. Nakauchi, N. Kawaguchi, and T. Yanagida: Jpn. J. Appl. Phys. **58** (2019) 052005. https://doi.org/10.7567/1347-4065/ab116c
24 H. Fukushima, D. Nakauchi, N. Kawaguchi, and T. Yanagida: J. Ceram. Process. Res. **20** (2019) 211. https://doi.org/10.36410/jcpr.2019.20.3.211
25 H. Fukushima, D. Nakauchi, T. Kato, N. Kawaguchi, and T. Yanagida: Radiat. Meas. **133** (2020) 106280. https://doi.org/10.1016/j.radmeas.2020.106280
26 H. Fukushima, D. Nakauchi, T. Kato, N. Kawaguchi, and T. Yanagida: Sens. Mater. **35** (2023) 429. https://doi.org/10.18494/SAM4139
27 M. Cao, J. Xu, C. Hu, H. Kou, Y. Shi, H. Chen, J. Dai, Y. Pan, and J. Li: Ceram. Int. **43** (2017) 2165. https://doi.org/10.1016/j.ceramint.2016.10.198
28 P. Lecoq: Nucl. Instrum. Methods Phys. Res., Sect. A **809** (2016) 130. https://doi.org/10.1016/j.nima.2015.08.041
29 D. Cavouras, I. Kandarakis, G. S. Panayiotakis, E. K. Evangelou, and C. D. Nomicos: Med. Phys. **23** (1996) 1965. https://doi.org/10.1118/1.597769
30 X.-Y. Sun, Y. Liu, X.-L. Liu, R.-P. Cao, Y.-N. Li, and L.-W. Lin: Opt. Mater. **36** (2014) 1478. https://doi.org/10.1016/j.optmat.2014.03.044
31 Y. Shi, Q. W. Chen, and J. L. Shi: Opt. Mater. **31** (2009) 729. https://doi.org/10.1016/j.optmat.2008.04.017
32 J. Fu, M. Kobayashi, S. Sugimoto, and J. M. Parker: Mater. Res. Bull. **43** (2008) 1502. https://doi.org/10.1016/j.materresbull.2007.06.024
33 W. Huang, Y. Li, J. Chen, Y. Zhao, L. Chen, and H. Guo: Ceram. Int. **49** (2023) 8863. https://doi.org/10.1016/j.ceramint.2022.11.042
34 S. Matsumoto, T. Watanabe, and A. Ito: Sens. Mater. **34** (2022) 669. https://doi.org/10.18494/SAM3698
35 C. Mansuy, J. M. Nedelec, C. Dujardin, and R. Mahiou: Opt. Mater. **29** (2007) 697. https://doi.org/10.1016/j.optmat.2005.10.017
36 C. LeLuyer, M. Villanueva-Ibañez, A. Pillonnet, and C. Dujardin: J. Phys. Chem. A **112** (2008) 10152. https://doi.org/10.1021/jp803339n
37 F. Khrongchaiyaphum, N. Wantana, S. Kansirin, P. Pakawanit, N. Vittayakorn, S. Kothan, N. Chanthima, H. J. Kim, and J. Kaewkhao: Optik **292** (2023) 171355. https://doi.org/10.1016/j.ijleo.2023.171355
38 S. Chen, Z. Wen, X. Peng, G. A. Ashraf, R. Wei, T. Pang, and H. Guo: Ceram. Int. **48** (2022) 947. https://doi.org/10.1016/j.ceramint.2021.09.179
39 T. Yanagida, K. Kamada, Y. Fujimoto, H. Yagi, and T. Yanagitani: Opt. Mater. **35** (2013) 2480. https://doi.org/10.1016/j.optmat.2013.07.002
40 T. Yanagida, Y. Fujimoto, T. Ito, K. Uchiyama, and K. Mori: Appl. Phys. Express **7** (2014) 062401. https://doi.org/10.7567/APEX.7.062401
41 A. Feteira, D. C. Sinclair, K. Z. Rajab, and M. T. Lanagan: J. Am. Ceram. Soc. **91** (2008) 893. https://doi.org/10.1111/j.1551-2916.2007.02134.x
42 Y. M. Ji, D. Y. Jiang, Z. H. Wu, T. Feng, and J. L. Shi: Mater. Res. Bull. **40** (2005) 1521. https://doi.org/10.1016/j.materresbull.2005.04.026
43 T. Kunikata, K. Watanabe, P. Kantuptim, K. Ichiba, D. Shiratori, T. Kato, D. Nakauchi, N. Kawaguchi, and T. Yanagida: Jpn. J. Appl. Phys. (2023). https://doi.org/10.35848/1347-4065/acfb16
44 K. Qin, J. Sun, X. Zhu, F. Cao, W. Liu, X. Shen, X. Wu, and Z. Wu: J. Lumin. **233** (2021) 117920. https://doi.org/10.1016/j.jlumin.2021.117920
45 H. Fukushima, D. Nakauchi, T. Kato, N. Kawaguchi, and T. Yanagida: J. Lumin. **223** (2020) 117231. https://doi.org/10.1016/j.jlumin.2020.117231
46 A. Maurya, A. Bahadur, and S. B. Rai: J. Lumin. **203** (2018) 714. https://doi.org/10.1016/j.jlumin.2018.07.025
47 G. A. Gusev, K. N. Orekhova, V. A. Kravets, A. I. Isakov, A. N. Trofimov, and M. V. Zamoryanskaya: J. Lumin. **222** (2020) 117084. https://doi.org/10.1016/j.jlumin.2020.117084
48 T. Yanagida: Proc. Jpn. Acad. Ser. B **94** (2018) 75. https://doi.org/10.2183/pjab.94.007
49 Q. Liu, Y. Yuan, J. Li, J. Liu, C. Hu, M. Chen, L. Lin, H. Kou, Y. Shi, W. Liu, H. Chen, Y. Pan, and J. Guo: Ceram. Int. **40** (2014) 8539. https://doi.org/10.1016/j.ceramint.2014.01.068
50 A. P. de Moura, L. H. Oliveira, I. C. Nogueira, P. F. S. Pereira, M. S. Li, E. Longo, J. A. Varela, and I. L. V. Rosa: Adv. Chem. Eng. Sci. **04** (2014) 374. https://doi.org/10.4236/aces.2014.43041
51 G. Gao, N. Da, S. Reibstein, and L. Wondraczek: Opt. Express **18** (2010) A575. https://doi.org/10.1364/OE.18.00A575